Title

A novel, soft edge microrough titanium surface to overcome osteoblasts kinetics dichotomy

Author

Vanjari, Gauri Kiran

Publication Date

2024

Peer reviewed|Thesis/dissertation

UNIVERSITY OF CALIFORNIA

Los Angeles

A novel, soft edge microrough titanium surface to overcome osteoblasts kinetics dichotomy.

Short title**:** Soft edge microrough titanium

A thesis submitted in partial satisfaction of the requirements for the degree Master of Science in Oral Biology

by

Gauri Kiran Vanjari

2024

ABSTRACT OF THE DISSERTATION

A novel, soft edge microrough titanium surface to overcome osteoblasts kinetics dichotomy.

by

Gauri Kiran Vanjari

Master of Science in Oral Biology

University of California, Los Angeles, 2024

Professor Takahiro Ogawa, Chair

Titanium implants are the standard therapeutic option for restoring missing teeth and reconstructing fractured or diseased bone. Despite the advancements in implant surface technology over the past 30 years, the osseointegration capabilities of titanium have not significantly improved. This study aimed to develop a novel microrough titanium surface with smooth, rounded edges to enhance osteoblast proliferation and differentiation while improving osseointegration [1,2,5].

In this study, the surface characterization involved flame-heating titanium surfaces thus transforming sharp, knife-like edges into smooth, rounded forms. Scanning Electron Microscopy (SEM) and Atomic Force Microscopy (AFM) were employed to visualize and quantify surface morphology changes. X-ray Photoelectron Spectroscopy (XPS) confirmed that the surface

chemistry remained consistent post-treatment. Wettability was assessed via water contact angle measurements, and cell attachment and proliferation were evaluated using WST-1 assays, fluorescent microscopy, BrdU incorporation, and flow cytometry.

Our findings indicated a substantial enhancement in osteoblast attachment and proliferation on the soft edge microrough surface compared to the knife-edge surface. The WST-1 assay, and fluorescent microscopy confirmed higher cell attachment on the newly created surface. Enhanced cell spreading behavior was observed, with larger cell area, perimeter, and Feret's diameter. Proliferation assays showed sustained increases in cell numbers, and BrdU incorporation confirmed higher DNA synthesis rates. Flow cytometric analysis indicated improved cell cycle progression.

Osteoblast differentiation and function were assessed through ALP activity, matrix mineralization assays, and gene expression analysis. Alizarin red staining demonstrated robust extracellular matrix formation and mineralization on the new surface. Gene expression analysis was also performed to compare the osteogenic potential.

Thus, we demonstrated that our novel micro- rough titanium surface generates substantially increased Osseo integrative ability over the previously available micro-rough titanium surface. This novel surface can have vivid applications in dental and orthopedic fields as well as titanium-based bone engineering scaffolds.

The thesis of Gauri Kiran Vanjari is approved.

Renate Lux

Alireza Moshaverenia

Takahiro Ogawa, Committee Chair

University of California, Los Angeles

2024

Dedication

To आजी (Grandmother), आजोबा (Grandfather), आई (Mom), बाबा (Dad), आत्या (Aunt),

ताई (Sister) and to all my true well-wishers

TABLE OF CONTENTS

ACKNOWLEDGEMENTS

I am immensely grateful to my advisor Dr. Takahiro Ogawa. I feel blessed to get the opportunity to work under his tutelage. Besides, I thank all my labmates, Dr. Keiji Komatsu, Dr. Takanori Matssuura and Dr. Toshikatsu Suzumura for their valuable feedback, timely help, guidance and comments on my work.

I am deeply indebted to all the committee members of my thesis defense committee Dr. Renate Lux and Dr. Alireza Moshaverenia for evaluating my work and being appreciative of my ideas and providing their valuable feedback. I am beyond words immensely grateful to Dr Wong for always being my cheerleader and motivator.

My sincere thanks are also due to my friends, and family friends that provided priceless social support during my program. I thank all my friends, including but not limited to Dr. Parag Surana, Dr. Umang Gandhi, Dr. Rewa Yadav, Dr. Nikhil Yadav, Dr. Prachi Dabholkar, Dr. Shivani Koli, Dr. Bharati Gitte, Dr. Heena W, Dr. Mrunali P, Dr. Natasha Shetty, Dr. Rutuja Vibhute, Abhishek Mathrani, Britjette Mayfield, Radha Lahoti, Amadea, Tripti Agarwal and Dr. Pradip Gatkine for their genuine concern, support, affection and for helping me when in need.

I now come to the part where I am expected to thank my parents, but how? They are the only *gurus* on earth whose unbounded and multi-dimensional blessings, love, support, and availability exist AND can be taken for granted. Thanking them adequately, therefore, is neither required nor possible! I consider myself a little extra lucky to have strongest support system in the form of my

Aunt Smt. Mangala M and my sister Dr. Vaishali M. who I have grown looking upto and it won't be incorrect to say that if it was not for them who knows where I would be today!

Many thanks to my teachers, Prof. Kedar Vaidya, Prof. Shridhar Shetty, Prof. Prashant Shetty, Prof. Premraj Jadhav, Prof. Sheetalkumar Sagari, Ms. Biji, Dr. Priyanka R, Dr. Yugandhara, and Ms.Sumathy, who have shaped me into who I am today.

Besides, I should also be grateful to my ancestors and my grandparents. Had they not done what they did, who knows what my family situation would have been today!

Last but far from least, I thank all those dreaded enemies called adversities. I abhor them all, but some of them lend me the raw oil that I need for that capricious flame called passion to blaze! And it's blazing! And I am alive!

Chapter 1. Introduction.

The utilization of titanium implants has become standard practice in bone, joint, and dental reconstruction within the fields of orthopedic surgery and dentistry. However, despite their widespread adoption, implant therapy continues to encounter numerous challenges. These challenges include the need for revision surgery, occurrences of surgical complications and infections, necessary use of acrylic bone cement to immobilize implants, prolonged healing periods, a plateaued success rate, and restricted indications due to various systemic factors and local anatomical considerations. These obstacles are intimately tied to insufficient bone formation volume and speed around implants. Notably, the reported percentage of bone coverage around implants, also known as bone-implant contact (BIC), hovers around 45% ± 16% [1, 2], or 50%–75% [2-5], significantly lower than the ideal 100% [2]. The underlying reasons why BIC fails to achieve full integration, irrespective of the duration of healing, remain unanswered.

Microrough titanium surfaces, commonly created through techniques such as acid-etching, alkaline treatment, oxidation, sandblasting, or their combinations, have emerged as the gold standard in implant surfaces and are widely utilized in both dental and orthopedic implants. These microrough surfaces exhibit micro-scale irregularities or roughness, characterized by peaks and valleys forming compartments ranging from 1-5 μm, albeit with variations in morphological features depending on the modification technique. Microrough surfaces offer several advantages: they enhance mechanical interlocking between implants and bone, promote osteogenic cell differentiation, and improve the quality of newly formed bone and interfacial molecular structure at implant surfaces [43, 47, 48] Consequently, the speed and strength of bone-implant integration or osseointegration are heightened around microrough surfaces compared to their machine-smooth

counterparts. However, a notable drawback of microrough surfaces is their reduced cell attachment, as well as suppressed cell motility, including diminished and delayed cellular spread and cytoplasmic projection, and more importantly, a decreased rate of cell proliferation. Consequently, the volume of bone generated around microrough surfaces is typically smaller than that observed around machine-smooth surfaces.

The proliferation and differentiation of osteoblasts represent a trade-off, with an inherent inverse correlation between these processes (**Figure 1**). For instance, when osteoblasts differentiate rapidly, they slow down their proliferation. Achieving optimal levels of both proliferation and differentiation simultaneously presents a significant challenge. Termed the "biological dilemma," this challenge is illustrated by the fact that on rough surfaces, osteoblasts proliferate at a slower rate but differentiate more rapidly, resulting in accelerated yet thinner bone formation [4, 6-10]. Conversely, on smooth surfaces, osteoblasts proliferate more rapidly but differentiate at a slower pace, leading to delayed osseointegration [6-8, 11-14]. This dichotomy is not unique to titanium but is observed across various biomaterials, complicating the development of bioactive surfaces. From a biomechanical standpoint, as mentioned earlier, implant surfaces typically need to be rougher to enhance mechanical interlocking with bone, which compromises cell proliferation. This inherent challenge underscores the ongoing difficulty in achieving complete osseointegration and explains the limited progress in implant surface technology over the past three decades. Current implant surfaces prioritize mechanical interlocking and osteoblastic differentiation, at the expense of the rate of osteoblast attachment and proliferation.

We hypothesized that the dichotomy in osteoblast kinetics could be mitigated by refining a surface feature while preserving the overall configuration of existing microrough surfaces. Specifically, microrough surfaces, as depicted in the illustration (**Figure 2**), feature sharp, knife-like edges that create micro-pits and compartments. By transforming these edges into smooth, rounded forms while maintaining consistent micro-compartments in terms of height and size, osteoblast proliferation could be enhanced compared to the knife-edge microrough surface, while still promoting accelerated differentiation. Here, we present the development of a novel microrough titanium surface with smooth, rounded edges, designed to enhance osteoblast attachment and proliferation compared to the commonly used microrough titanium surface with knife-edges. These findings offer a fresh perspective on overcoming the osteoblast kinetics dichotomy and present a pioneering strategy for the advancement of more effective implant surfaces.

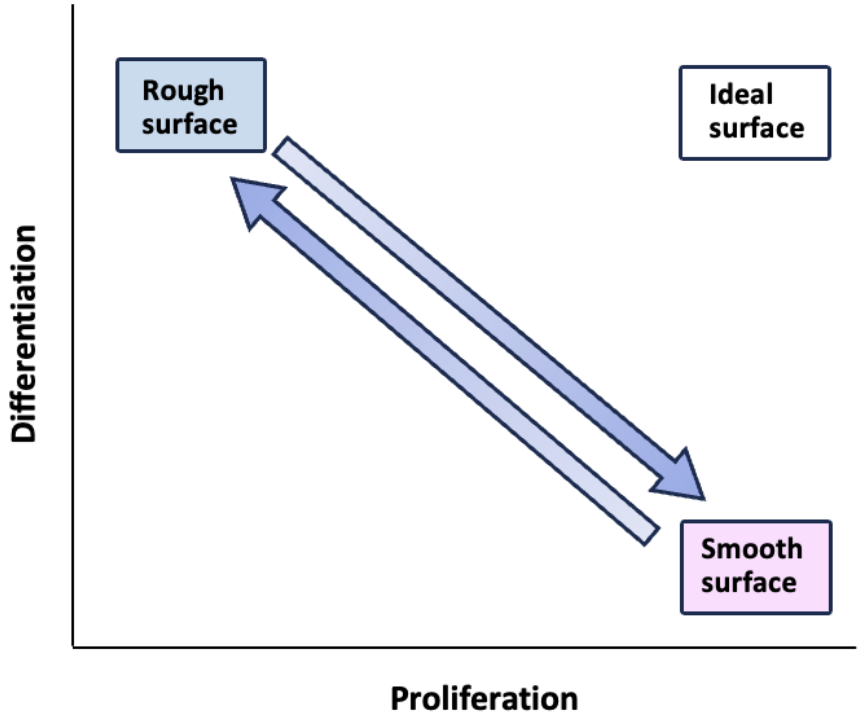

Figure 1

Dichotomy of osteoblast kinetics on different implant surfaces. Osteoblast kinetics encompass the critical processes of proliferation and differentiation, which are inversely correlated. When osteoblast differentiation is promoted, proliferation is suppressed, and vice versa. On rough implant surfaces, such as microrough surfaces, osteoblasts differentiate more rapidly but proliferate more slowly. Conversely, on smooth implant surfaces, such as machined surfaces, osteoblasts proliferate more quickly but their differentiation is delayed. Achieving a surface that promotes both proliferation and differentiation remains a significant challenge in implant science and therapy.

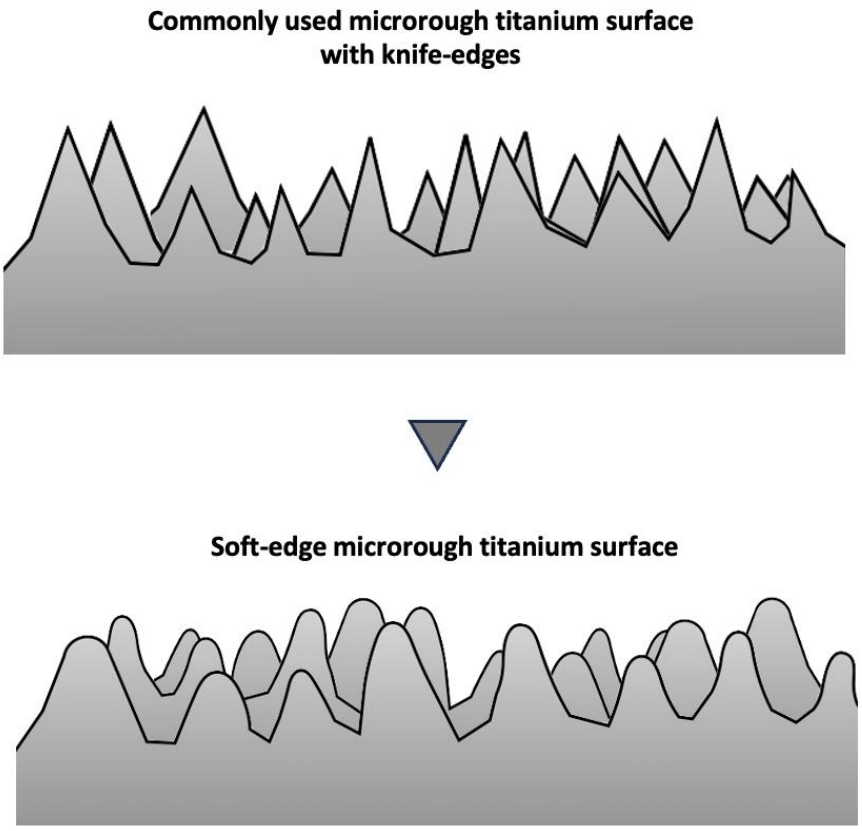

Figure 2

Strategy to mitigate the unfavorable dichotomy of osteoblast kinetics by modifying microrough titanium surfaces. Currently used microrough surfaces, typically crafted through acid-etching, feature micro-scale compartmental structures formed by sharp, knife-edge-like peaks (top panel). While osteogenic cells differentiate faster on these rough surfaces, their proliferation is significantly compromised, leading to rapid bone formation but reduced bone volume around implants. This study hypothesized that transforming these knife-edges into soft edges (bottom

panel) could alleviate the reduction in proliferation while preserving the enhanced differentiation. Note that that the general configuration of peaks and compartmental structures remain unchanged.

Chapter 2 Specific Aims:

Aim 1: To Characterize and Optimize the Surface Morphology of Titanium Implants Using Flame-Heating

Rationale: Surface morphology plays a crucial role in the interaction between implants and surrounding bone tissue. Modifying the surface to achieve a balance between roughness for better integration and smoothness to avoid adverse cellular responses can enhance implant performance.

Objective 1.1: Utilize flame-heating to modify the surface morphology of titanium implants, transforming sharp microrough edges into smooth, rounded forms.

Objective 1.2: Conduct surface characterization using scanning electron microscopy (SEM), atomic force microscopy (AFM), and X-ray photoelectron spectroscopy (XPS) to analyze the changes in surface topography and chemical composition.

Objective 1.3: Assess the wettability of the modified surfaces through water contact angle measurements to correlate surface morphology with wettability, which influences cell attachment and proliferation.

Aim 2: To Evaluate the Impact of Surface Morphology on Osteoblast Attachment and Proliferation

Rationale: The initial cellular response to implant surfaces, including attachment and proliferation, is critical for successful osseointegration. Understanding how different surface morphologies affect these processes can guide the design of better-performing implants.

Objective 2.1: Compare osteoblast attachment on soft-edge microrough surfaces and conventional knife-edge microrough surfaces using WST-1 assays and fluorescent microscopy.

Objective 2.2: Analyze cell spreading behavior, including cell area, perimeter, and Feret's diameter, to assess the effects of surface morphology on cytoskeletal organization.

Objective 2.3: Measure osteoblast proliferation on different surface types using WST-1 assays, BrdU incorporation, and flow cytometry to evaluate cell cycle progression and proliferation rates.

Aim 3: To Investigate Osteoblast Differentiation and Function on Modified Titanium Surfaces

Rationale: Beyond initial attachment and proliferation, osteoblast differentiation and function are essential for long-term implant success. Assessing differentiation markers and matrix mineralization will provide insights into the osteogenic potential of different surface morphologies.

Objective 3.1: Evaluate early osteoblastic differentiation by measuring alkaline phosphatase (ALP) activity on soft-edge and knife-edge microrough surfaces.

Objective 3.2: Perform matrix mineralization assays using Alizarin red staining to assess extracellular matrix formation on different surface types.

Objective 3.3: Conduct qPCR analysis to quantify the expression of osteoblastic markers (e.g., type I collagen, osteopontin, osteocalcin, BMP-2) on modified surfaces, determining the impact of surface morphology on osteogenic gene expression.

Aim 4: To Assess In Vivo Osseointegration of Soft-Edge Microrough Titanium Implants

Rationale: In vivo performance is the ultimate test of an implant's effectiveness. Evaluating osseointegration through biomechanical tests will validate the benefits of surface modifications observed in vitro.

Objective 4.1: Implant soft-edge and knife-edge microrough titanium implants in a rat femur model and conduct biomechanical push-in tests to measure push-in force and stiffness.

Objective 4.2: Use SEM to analyze the bone-implant interface, assessing bone-implant contact and integration.

Objective 4.3: Correlate in vivo findings with in vitro results to understand the mechanisms underlying enhanced osseointegration on soft-edge microrough surfaces.

Chapter 3. Materials and methods

3.1. Titanium specimens, surface modification, and surface characterization

Titanium specimens in a disk form (20 mm diameter and 1 mm thickness) were prepared by machine-milling grade 2 commercially pure titanium. To create a conventional microroughness, the disks were acid-etched by H_2SO_4 at 95°C for 3 minutes. To round the sharp edges of the microrough surfaces, we attempted to flame-heat the disks for varying time duration, 12, 22, and 32 seconds. The disks turned into a red-hot state at 22 seconds.

All specimens were sterilized by autoclaving before cell culture. Surface morphology was examined by scanning electron microscopy (SEM; Nova 230 Nano SEM, FEI, Hillsboro, Oregon) and an optical profile microscope (MeX, Alicona Imaging GmbH, Raaba, Graz, Austria) for quantitative roughness analysis. The average roughness (Sa), peak-to-valley roughness (Sz), developed interfacial area ratio (Sdr), root mean square gradient (Sdq), kurtosis (Sku), peak density (Spd), arithmetic mean peak curvature (Spc), core void volume (Vcc), and core height (Sk) were calculated. Surface chemical composition was determined by X-ray photoelectron spectroscopy (XPS) (Axis Ultra DLD spectrometer, Kratos Analytical, Shimadzu, Kyoto, Japan) and the hydrophilicity/hydrophobicity of the surfaces was evaluated by measuring the contact angle of 3 μL ddH_2O.

3.2. Osteoblast culture

As described elsewhere[15-19], bone marrow-derived osteoblasts were isolated from the femurs of 10-week-old male Sprague–Dawley rats and placed into alpha-modified Eagle's medium

supplemented with 15% fetal bovine serum, 50 µg/ml ascorbic acid, 10 mM Na-ß-glycerophosphate, 10^{-8} M dexamethasone, and antibiotic–antimycotic solution containing 10,000 units/ml penicillin G sodium, 10,000 mg/ml streptomycin sulfate, and 25 mg/ml amphotericin B. Cells were incubated in a humidified atmosphere of 95% air and 5% CO_2 at 37°C. At 80% confluency, the cells were detached using 0.25% trypsin–1 mM EDTA-4Na and seeded onto titanium disks placed in 12-well culture dishes at a density of 2×10^4 cells/cm^2. The culture medium was renewed every three days. All experiments were performed following protocols approved by The Chancellor's Animal Research Committee at the University of California at Los Angeles (ARC #2005-175-41E, approved January 30, 2018), the PHS Policy for the Humane Care and Use of Laboratory Animals, and the UCLA Animal Care and Use Training Manual guidelines.

3.3. Osteoblast attachment and proliferation assays

The number of osteoblasts attached to titanium surfaces during the initial stage of culture was evaluated using a tetrazolium salt (WST-1)-based colorimetric assay (WST-1; Roche Applied Science, Mannheim, Germany) on day 1 of culture as described elsewhere [11, 20-22]. To evaluate the proliferative activity of osteoblasts, the density of propagated cells was also quantified using a WST-1 assay on day 4. The proliferative activity of osteoblasts was also confirmed by 5-bromo-2'-deoxyuridine (BrdU) incorporation during DNA synthesis. On day 4, 100 ml of 100 mM BrdU solution (Roche Applied Science, Mannheim, Germany) was added to the culture wells followed by incubation for 10 h. After trypsinizing the cells and denaturing the DNA, cultures were incubated with peroxidase-conjugated anti-BrdU for 90 min and reacted with tetramethylbenzidine for color development. Absorbance at 370 nm was measured using an ELISA plate reader (Synergy HT, BioTek Instruments, Winooski, VT, USA).

3.4. Morphology and spreading behavior of osteoblasts

The cell morphology was visualized and evaluated by fluorescence microscopy (DMI 4000 B, Leica Microsystems Inc., Buffalo Grove, IL, USA). On day 1 of culture, osteoblasts were fixed with 10% formalin and stained with 4′,6-diamidino-2-phenylindole (DAPI, Vector Laboratories, Burlingame, CA, USA) for nuclei and rhodamine phalloidin for actin filaments (Molecular Probes, Eugene, OR, USA). The area, perimeter, and Feret's diameter of cells were measured using ImageJ (ver.1.51j8, NIH, Bethesda, MD, USA).

3.5. Cell cycle analysis

To validate the modulated cell proliferation on different titanium surfaces, we conducted a cell cycle analysis using Cell Cycle Assay Solution Blue (Dojindo Laboratories, Kumamoto, Japan), as reported elsewhere[23]. Briefly, osteoblasts cultured on titanium disks were collected on day 2 and incubated with 5 μL of the assay solution at 37 ◦C for 15 min. The DNA content was subsequently determined using a Gallios flow cytometer (Beckman Coulter, Miami, FL, USA). Then, cell distribution in the G1, S, and G2 phases was analyzed, and the G2/G1 and S/G1 ratios were calculated.

3.6. Alkaline phosphatase (ALP) activity

The ALP activity is a representative cellular phenotype during the early stage of osteoblastic differentiation. As reported previously [24, 25], the cultured samples at day 4 were rinsed with

double-distilled water (ddH2O) and treated with 250 μL p-nitrophenylphosphate (Wako Pure Chemicals, Richmond, VA, USA) and further incubated at 37 ◦C for 15 min. ALP activity was evaluated as the amount of nitrophenol released through the enzymatic reaction and measured at a wavelength of 405 nm using a microplate reader.

3.7. Matrix mineralization assay

Extracellular matrix mineralization is a final-step functional events representing osteoblastic differentiation. Alizarin red stain was used to detect the mineralized matrix. As reported elsewhere [26-29], on day 10, cultures were washed three times with PBS and fixed in 10 % formalin for 10 min before being stained with 1 % alizarin red solution (Sigma-Aldrich, St. Louis, MO, USA) for 5 min at room temperature. The dyed samples were dissolved in 10 % acetic acid for 30 min before adding 200 μl 10 % ammonium hydroxide to neutralize the acid. The optical density was measured at 405 nm using a microplate reader.

3.8. Real-time quantitative polymerase chain reaction (qPCR)

As described elsewhere[24, 30-32], the expression of osteoblastic differentiation maker genes was analyzed using qPCR on day 4. Total RNA was extracted from cells using TRIzol (Invitrogen, Carlsbad, CA, USA) and a Direct-zol RNA MiniPrep kit (Zymo Research, Irvine, CA, USA). Extracted RNA was reverse transcribed into first-strand cDNA using SuperScript III Reverse Transcriptase (Invitrogen). Quantitative PCR was performed in a 20 μL volume containing 90 ng cDNA, 10 μL TaqMan Universal Master Mix II, and 1 μL TaqMan Gene Expression Assay using a QuantStudio 3 Real-Time PCR System (Thermo Fisher Scientific, Canoga Park, CA, USA), to

quantify the expression of type I collagen, osteopontin, osteocalcin, and BMP 2 mRNA. *Gapdh* expression was used as the endogenous control.

3.9. Implant surgery.

As described elsewhere [13, 14, 33-35], eight-week-old male Sprague–Dawley rats were anesthetized by inhalation with 1%–2% isoflurane. After their legs were shaved and scrubbed with 10% povidone-iodine solution, the distal aspects of the femurs were carefully exposed through skin incision and muscle dissection. The flat surfaces of the distal femurs were selected for implant placement. The implant site was prepared 11 mm from the distal edge of the femur by drilling with a 0.8 mm round burr and enlarged using reamers (#ISO 090 and 100). One cylindrical implant, with either a knife-edge microrough surface or a soft edge microrough surface, was placed into one femur, alternating the side for each group of implants. Surgical sites were then closed in layers, with muscle and skin sutured separately using resorbable sutures.

3.10. Implant biomechanical push-in test.

The biomechanical capacity of bone-implant interface to withstand a load is the most pertinent variable to evaluate the implant as an anchoring device. The established implant biomechanical push-in test was used to assess the strength of bone–implant integration[11, 20, 36-41]. At week 2 of healing, femurs containing a cylindrical implant were harvested and embedded into auto polymerizing resin with the top surface of the implant parallel to the ground. A testing machine (Instron 5544 electro-mechanical testing system, Instron, Canton, MA, USA), equipped with a 2,000 N load cell and a pushing rod (0.8 mm in diameter), was used to load the implant vertically

downward into the bone marrow at a crosshead speed of 1 mm/min. The yield strength, elastic modulus, resiliency, and energy of osseointegration were determined from the load–strain curves.

3.11. Morphological and elemental analyses of implant/tissue complex

Morphological and elemental analyses of implant surfaces after the biomechanical push-in test have proven useful for interpreting the properties of osseointegration and its failure[36, 42]. After the push-in test at week 2 of healing, the implants were carefully exposed, soaked in agitated water for one hour, and dried under heat and vacuum. The specimens were then examined by scanning electron microscopy (SEM). The elemental composition of the tissue remnants and the implant interface were analyzed by energy dispersive X-ray spectroscopy (EDX) (UltraDry EDS Detector and Noran System 6, Thermo Fisher Scientific).

3.12. Statistical analyses

Data on surface roughness parameters were collected from six sites on multiple disks ($n = 6$). Three disks were used for all cell culture studies and physicochemical characterization ($n = 3$). One-way ANOVA was performed to examine the differences among differently textured surfaces. When appropriate, Bonferroni's test was used as a post-hoc test. For comparisons between two surfaces, a non-paired t-test was used. P-values less than 0.05 were considered statistically significant.

Chapter 4. Results.

4.1. Creation and optimization of soft-edge microrough titanium surface (Specific Aim 1)

Our initial objective was to validate our technical hypothesis regarding the transformation of conventional knife-edge microrough titanium surfaces into surfaces with smooth edges through flame-heating. As illustrated in Figure 2, we theorized that heating microrough titanium surfaces would alter their structure, starting from the apex due to their smaller volume. Our technical approach involved selectively melting only the tips of the peaks while preserving the majority of the surface structures to maintain the micro-compartments. In the first step, grade 2 commercially pure titanium disks (Figure 3A) underwent acid-etching with sulfuring acid to generate microrough surfaces. Subsequently, the microrough titanium was subjected to flame-heating, with heating times ranging from 12 to 32 seconds. The titanium disk attained a red-hot state at 22 seconds (Figure 3B).

As expected, SEM images showed that the acid-etched titanium exhibited a typical micro-scale texture characterized by peaks and valleys, forming micro-pits or compartments ranging from 1 to 5 μm (Figure 3C). The peaks displayed sharpness, thus defining the surface as a knife-edge microrough surface. Upon flame-heating the microrough titanium, the knife-edges were indeed transformed into rounded shapes, a transformation dependent on the duration of heating. The degree of roundness progressed notably from 12 to 32 seconds, with the 32-second heating period

resulting in substantial melting of the peak structure and reduction in height. Consequently, the compartmental feature of the original microrough surface became less pronounced. However, heating durations of 12 and 22 seconds successfully preserved the compartmental configuration while rounding the edges, thereby establishing soft-edge microrough titanium surfaces. Optical microscopic 3-D images confirmed that the sharp edges of the original acid-etched surface were rounded by flame-heating, correlating with the heating time (bottom images in Figure 3C).

Quantitative roughness analysis unveiled both proportional and disproportional changes in variables reflecting morphological alterations following flame-heating for various durations (Figure 3D). Sa (average roughness) exhibited an increase on flame-heated titanium compared to the acid-etched, knife-edge microrough surface, with a progressive rise in heating time until 22 seconds, followed by a decrease at 32-second heating. Sz (maximum height) remained unchanged with flame-heating, except for a reduction after 32 seconds, while Sdr (developed interfacial ratio), representing surface area, followed a similar trend. Sdq (root mean square gradient) decreased after 22 and 32 seconds of heating, indicating a milder peak slope compared to the original knife-edge microrough surface. Sku (kurtosis) and Spc (peak curvature), representing peak sharpness or roundness, were notably lower on surfaces heated for 22 and 32 seconds compared to the original microrough surface, indicating softening of these peaks quantitatively. Spd (peak density) remained constant up to 22 seconds of heating. Both Vvc (dale void volume) and Sk (core height), representing spacious variables between structures, exhibited a correlated increase with heating time, peaking at 22 seconds.

The objective of refining the existing microrough surface was to round the edges while preserving or enhancing the existing morphological features. Flame-heating for 12 seconds did not appear to significantly round the edges, as indicated by the unaffected Sku and Spc. Additionally, the sustained Sdq confirmed that the peak structure was not significantly melted during the 12-second heating. Consequently, there was no significant increase in Vvc and Sk on this surface. In contrast, a significant decrease in Sku and Spc was observed after 22 seconds of heating, indicating successful edge rounding. Remarkably, this 22-second heating did not adversely affect Sa and Sz, and even led to a significant increase in Sa. Furthermore, Vvc and Sk exhibited significant increases on this surface. Although the 32-second heating caused significant melting of the peaks, as evidenced by decreased Sku and Spc, it also resulted in decreased Sa, Sz, and Sdr, suggesting a substantial melting of the peak structures and blurring of the microrough compartmental configuration. Thus, we identified the optimal flame-heating time of 22 seconds to create a soft-edge microrough titanium surface.

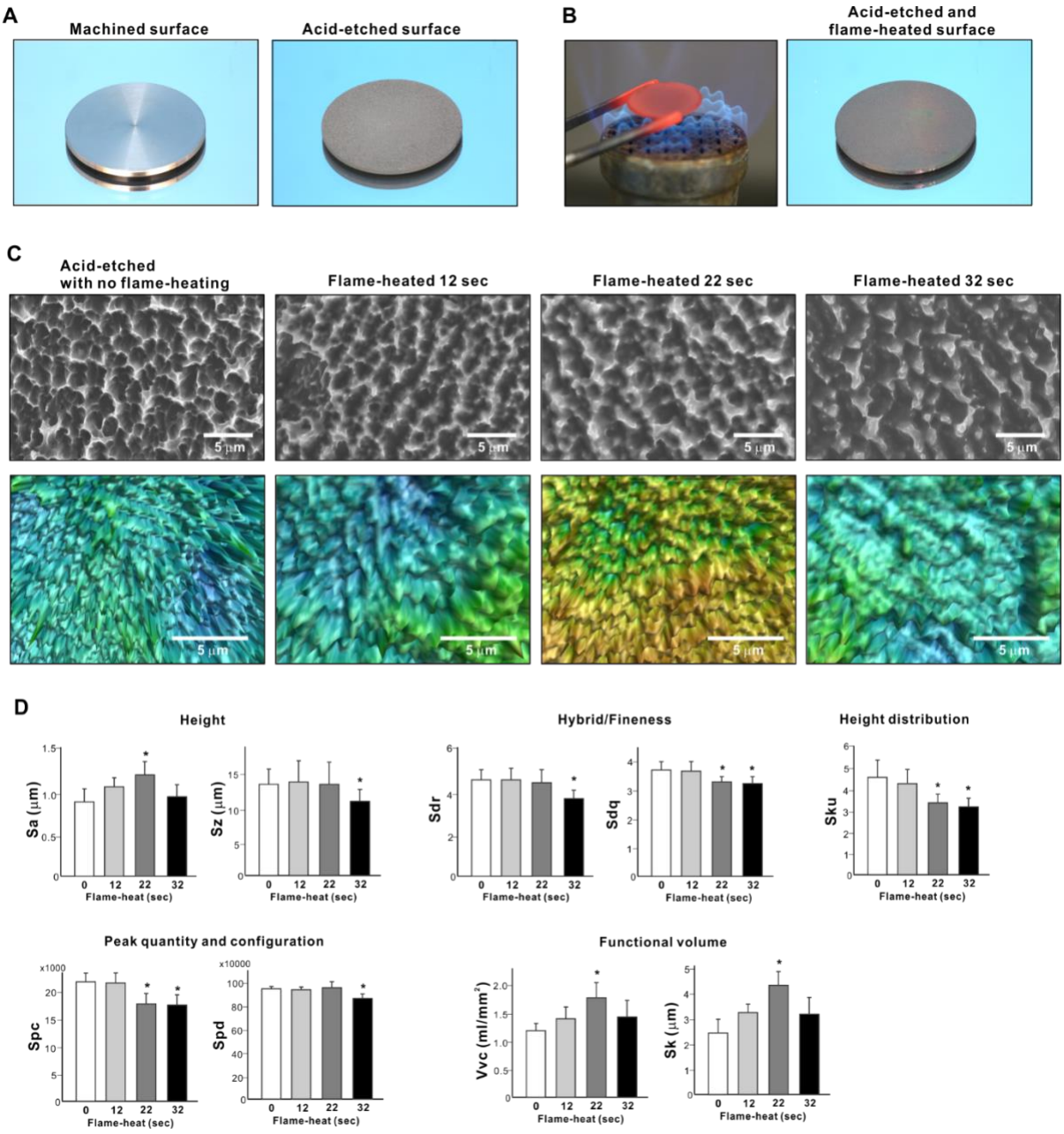

Figure 3

Optimization of the knife-edge to soft-edge conversion on microrough titanium surfaces. (A) Grade 2 commercially pure titanium disks used in the study. The disks were acid-etched with sulfuric acid to create a microrough surface. (B) Flame-heating of the microrough titanium disks for various durations aimed at rounding the knife-edge peaks of the original microrough surface.

(C) Scanning electron microscopic (SEM) images (top panels) and 3-dimensional confocal microscopic images (bottom panels) of the original microrough surface and flame-heated microrough surfaces for different durations. (D) Surface texture parameters of the surfaces evaluated by 3D laser scanning confocal microscope: Sa (average roughness), Sz (peak-to-valley roughness), Sdr (developed interfacial area ratio), Sdq (root mean square gradient), Sku (kurtosis), Spc (peak curvature), Spd (peak density), Vvc (core void volume), and Sk (core height). Statistically significant different from the original microrough surface (unheated): *$p < 0.05$; **$p < 0.01$; ***$p < 0.001$.

4.2. Physicochemical surface characterization of the soft edge microrough titanium

We then opted to utilize the 22-second flame-heated surface as an optimized soft-edge microrough titanium surface. To assess the biological efficacy of the soft-edge microrough surface and ascertain whether it overcomes the drawbacks of the conventional microrough surface, a comparative analysis was conducted between the soft-edge microrough surface, original acid-etched, knife-edge microrough surfaces, and machine-smooth surfaces. Prior to the biological evaluation, their physicochemical properties were characterized.

The machined titanium surfaces exhibited no discernible texture apart from the scratches and traces resulting from machine milling, as depicted in the SEM image (Figure 4A). AFM profiling revealed that the peaks that were sharp on the acid-etched surface were effectively rounded after flame-heating (black arrowheads in Figure 4B). In addition, peak structures were tempered after flame-heating, with their slopes was less steep. This was consistent with the reduced Sdq on the flame-heated surfaces, also contributed to an increase of inter-peak space.

XPS chemical analysis exhibited that the flame-heating reduced the percentage of surface oxygen and increased the surface carbon compared to the original acid-etched microrough surface (Figure 4C). Wettability assessment revealed that the contact angle was similar between the knife-edge and soft edge microrough surfaces, indicating that both surfaces exhibited hydro repellent

properties (defined as $\theta > 90°$). The contact angle of the machine-smooth surface was notably lower, signifying its hydrophobic nature (defined as $\theta > 60°$).

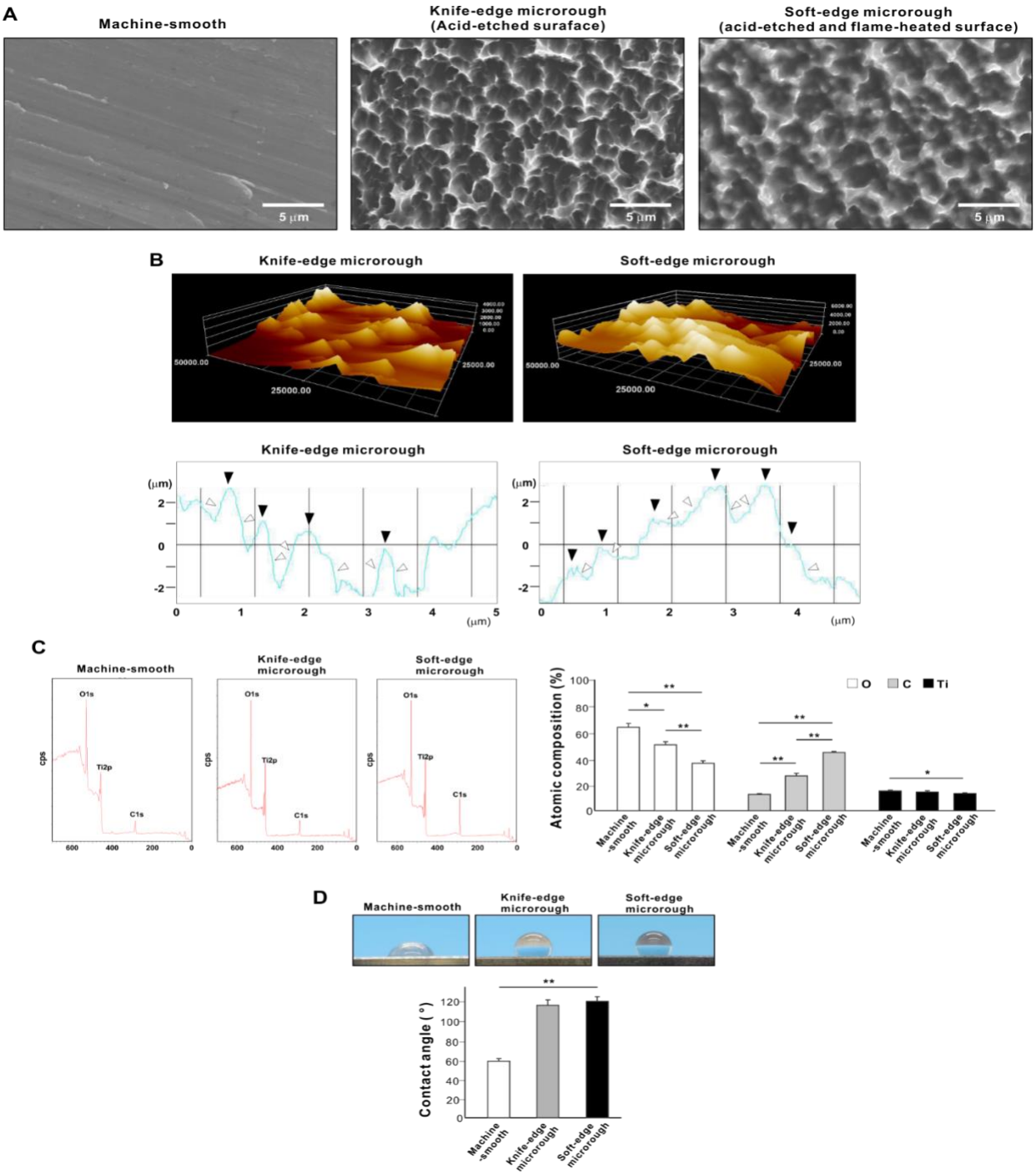

Figure 4

Surface characterization of three distinct titanium disks: machine-smooth surface, knife-edge microrough surface (acid-etched surface), and soft-edge microrough surface. Based on optimization results detailed in Figure 3, the soft-edge microrough surface, achieved by flame-

heating the acid-etched surface for 22 seconds, was selected. (A) Scanning electron microscope (SEM) images depicting the three surface types. (B) Atomic force microscopy (AFM) 3D images and representative profiling oscillation curves revealing the featured morphology of knife-edge and soft edge microrough surfaces. Black arrowheads highlight the difference between sharp peaks on the knife-edge surface and rounded peaks on the soft-edge surface. White arrowheads indicate the steep inclines of peaks on the knife-edge surface, which were tempered on the soft-edge surface. C) X-ray photoelectron spectroscopy (XPS) chemical analysis of machine-smooth, knife-edge, and soft-edge microrough surfaces. Representative XPS spectrum and atomic percentages of oxygen, carbon, and titanium elements are presented. (D) Wettability assessment of the three surfaces by droplet deposition of 3 μl of ddH2O. Statistically significant differences: *$p < 0.05$; **$p < 0.01$; ***$p < 0.001$.

4.3. Osteoblast initial behavior and growth on the soft edge microrough titanium (Specific Aim 2 and 3)

Within 24 hours of seeding, the number of osteoblasts attached to titanium notably decreased (approximately by half) on the original acid-etched microrough surface with knife-edges compared to the machine-smooth surface (Figure 5A). However, this diminished cell attachment was significantly reversed on the soft edge microrough surface. Fluorescent microscopic images confirmed the order of attached cells, with machine-smooth, soft-edge microrough, and knife-edge microrough surfaces, respectively. Not only did the number of cells differ, but also the altered shape and size of the cells prompted us to conduct cytomorphometry on these microscopic images. The area, perimeter, and Feret diameter of osteoblasts, which were notably reduced on the knife-edge microrough surfaces compared to the machine-smooth surfaces, were consistently restored on the soft-edge microrough surfaces, with improvements in perimeter and Feret diameter (Figure 5B).

The number of cells propagated until the subsequent culture day of 4 on the soft-edge microrough surface was significantly higher than on the knife-edge microrough surface, although still lower than that on the machine-smooth surface (Figure 5C). This observation was visually supported by microscopic images depicting extensive cell colonization and cluster formation on the soft edge microrough surface. Additionally, actin expression appeared more extensive and intense on the soft edge microrough surface compared to the knife-edge microrough surface. BrdU incorporation into DNA on day 4 confirmed that the cell proliferation rate on the soft edge microrough surface increased compared to the knife-edge microrough surface, reaching a level equivalent to that on the machined surface (Figure 5D).

We further analyzed the distribution of cells in each phase of cell proliferation on day 2. The machine-smooth surface, associated with the most robust cell proliferation, exhibited the lowest percentage of cells in the G1 phase, while the knife-edge microrough surface, linked to the most suppressed cell proliferation, showed the highest percentage (Figure 5E). The G1 phase percentage on the soft edge microrough surface fell between these two extremes. In contrast, the decrease in the percentage of cells in the S and G2 phases on the knife-edge microrough surface compared to the machine-smooth surfaces was mitigated on the soft-edge microrough surface. Consequently, osteoblasts on the soft-edge microrough surface displayed higher G2/G1 and S/G1 ratios than those on the knife-edge microrough surface and were closer to those on the machine-smooth surface. These findings indicate that the reduced osteoblast proliferation observed on the knife-edge microrough surface compared to the machine-smooth surface was considerably mitigated on the soft-edge microrough surface.

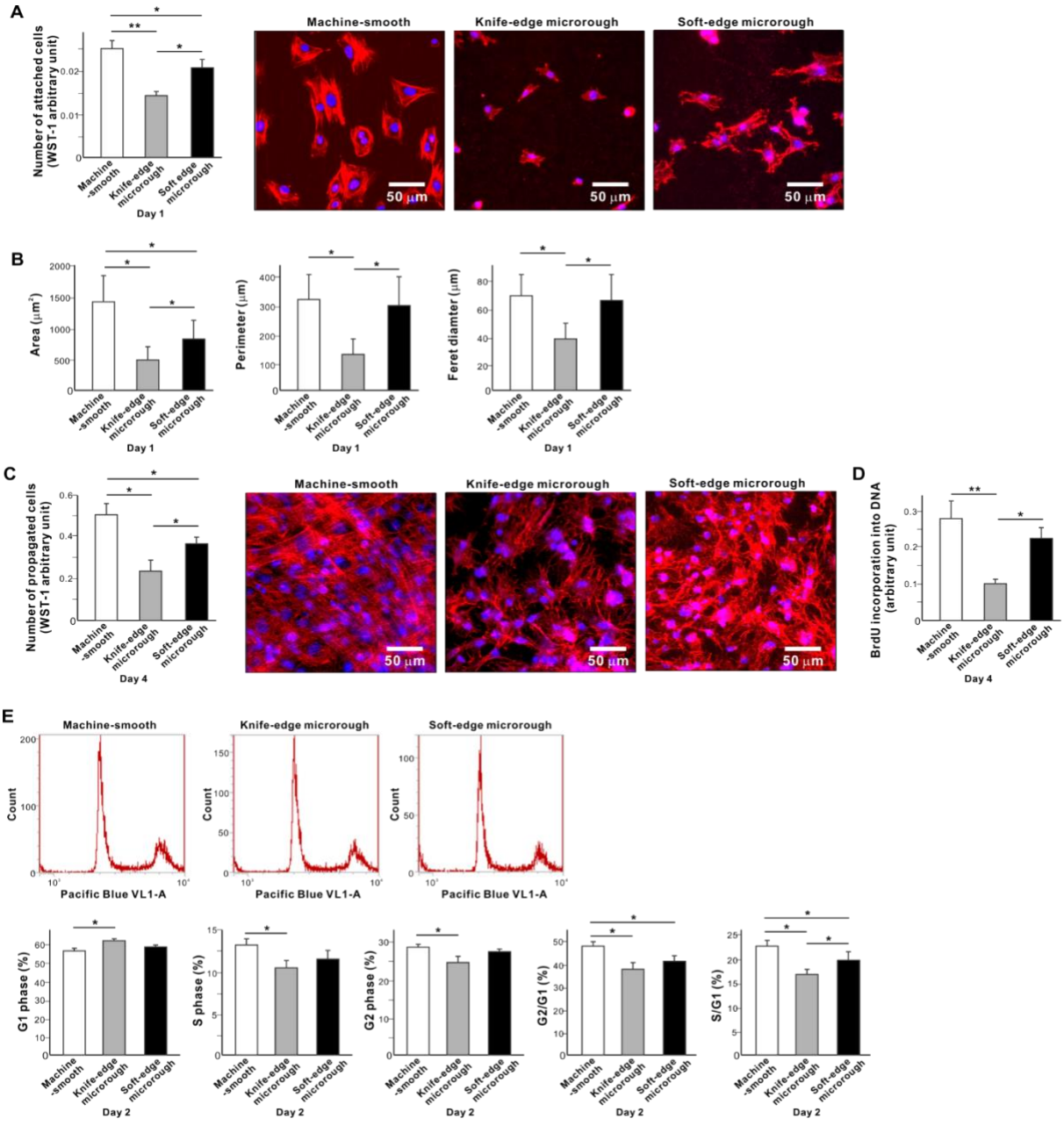

Figure 5

The attachment, initial behavior, and proliferation of osteoblasts on three distinct titanium surfaces: machine-smooth surface, knife-edge microrough surface (acid-etched surface), and soft-edge microrough surface. (A) The number of osteoblasts attached to titanium surfaces, evaluated

by WST-1 assay after 1 day of culture, along with fluorescent microscopic images. (B) Cytomorphometry conducted on culture day 1 based on the fluorescent microscopic images. (C) The number of osteoblasts propagated on titanium surfaces, evaluated by WST-1 assay on day 4, along with fluorescent microscopic images. (D) The proliferative activity of osteoblasts, evaluated on day 4 via BrdU incorporation into DNA. (E) Flow cytometric analysis of cell cycles and calculated distribution of osteoblasts in G1, S, and G2 phases, as well as the ratios G2/G1 and S/G1. Statistically significant differences: *$p < 0.05$; **$p < 0.01$; ***$p < 0.001$.

4.4. Osteoblast differentiation on the soft edge microrough titanium

We next delved into the functional differentiation of osteoblasts across the three different surfaces. Total ALP activity was highest on the soft-edge microrough surface and lowest on the knife-edge microrough surface, while ALP activity standardized by the number of cells was highest on the soft-edge microrough surface and lowest on the machine-smooth surface (Figure 6A). Mineralized matrix formation was also highest on the soft-edge microrough surface and lowest on the machine-smooth surface (Figure 6B). The expression level of osteoblastic differentiation marker genes consistently demonstrated higher levels on the microrough surfaces than on the machine-smooth surface, with no significant difference between the knife-edge and soft edge microrough surfaces (Figure 6C). These results indicate that osteoblast differentiation was not compromised and was even enhanced on the soft-edge microrough surface compared to that on the knife-edge microrough surface.

4.5. in vivo osseointegration to soft-edge microrough titanium (Specific Aim 4)

The biomechanical push-in test generated typical load-strain curves during compressive fracture testing for both knife-edge and soft-edge microrough implants (Figure 6D)[44,46,49]. The yield strength of osseointegration around soft edge microrough implants was approximately double that around knife-edge microrough implants (Figure 6E). Additionally, the elastic modulus was 1.6 times higher for implants with soft edge microrough surfaces. The resiliency and energy of osseointegration were more than twice as high for the soft edge microrough surfaces compared to the knife-edge microrough surfaces.

SEM images of implants after the push-in test revealed extensive bone coverage around the soft-edge microrough surfaces, whereas only a limited area of the knife-edge microrough surfaces exhibited remaining bone (Figure 6F). In addition to the increased area of bone coverage, the bone around the soft-edge microrough surfaces appeared three-dimensionally robust.

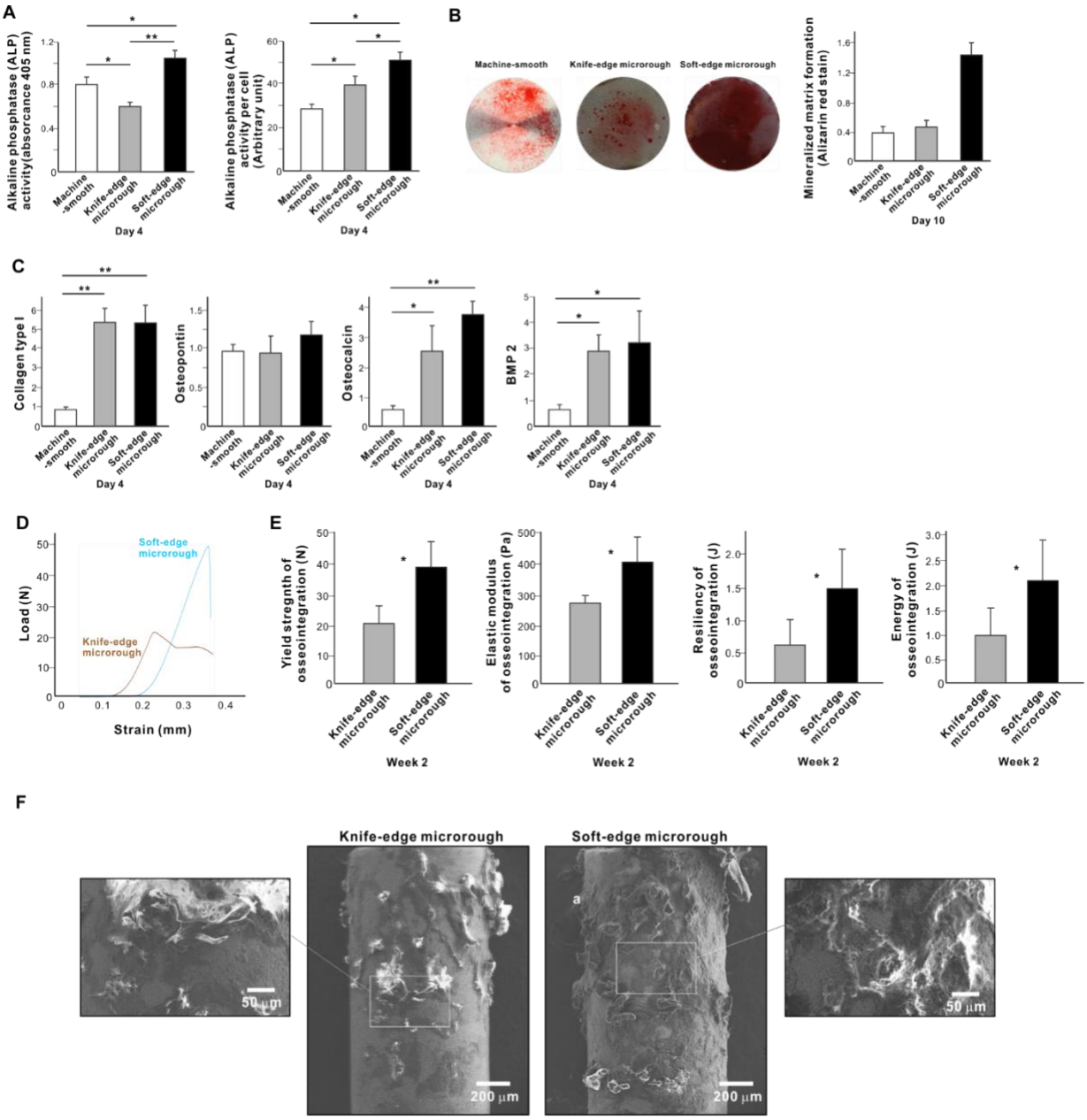

Figure 6

The functional differentiation of osteoblasts and in vivo osseointegration behaviors on three distinct titanium surfaces: machine-smooth surface, knife-edge microrough surface (acid-etched surface), and soft-edge microrough surface. (A) Alkaline phosphatase activity evaluated on day 4 with or without standardization relative to the number of cells. (B) Formation of mineralized

matrix evaluated by Alizarin red stain on day 10. (C) Expression levels of osteoblastic differentiation marker genes on day 4 evaluated by real-time qPCR. (D) Typical load-strain curves obtained through in vivo implant biomechanical push-in test in the rat femur, comparing knife-edge microrough and soft-edge microrough implants. (E) Mechanical property parameters of osseointegration calculated from the load-strain curves. (F) SEM images of implants retrieved after the biomechanical push-in test. Statistically significant differences: *$p < 0.05$; **$p < 0.01$; ***$p < 0.001$.

Chapter 5: Discussion:

The conventional microrough surfaces, characterized by sharp, knife-like edges, enhance osteoblast differentiation but impede proliferation, resulting in a compromise between the speed and volume of bone formation. By modifying these knife-edges to soft, rounded forms, we hypothesized that osteoblast proliferation could be improved without sacrificing differentiation [51-53].

The study aimed to transform conventional knife-edge microrough titanium surfaces into smooth-edged surfaces through flame-heating, with the goal of improving their morphological characteristics while maintaining the essential micro-compartmental features. Our findings demonstrated that flame-heating for specific durations successfully rounded the sharp edges of microrough surfaces, with an optimal heating time of 22 seconds yielding the most desirable results.

Weinlaender et al. (1992) evaluated bone apposition around different types of dental implants and found that surface roughness plays a crucial role in osseointegration. Our study complements these findings by demonstrating that flame-heating can modify surface roughness, potentially enhancing bone integration. In a systematic review conducted by Chambrone et al. (2020) the importance of bone titanium interface was emphasized in addition to surface characteristics. Our technique offers a novel approach to surface modification that preserves micro-compartments while rounding sharp edges, which improve biological responses . Ogawa et al. (2003) highlighted differences in bone integration profiles of acid-etched implants, showing that acid-etching enhances bone response .

Our results extend this by demonstrating that flame-heating acid-etched surfaces can further optimize the roughness parameters, potentially improving bone healing outcomes. Zhao et al. (2005), proved that high surface energy enhances cell response to titanium substrate microstructure, which is reiterated by our findings where flame-heating up to 22 seconds increases average roughness (Sa) suggesting that the increased surface energy may contribute to better cellular responses . Bachle and Kohal (2004) reviewed the influence of titanium surface roughness on osteoblast-like cell proliferation and differentiation . The rounded edges achieved through our flame-heating method promote similar cellular behaviors by providing a more conducive surface for cell attachment and proliferation. Our results indicate that flame-heating for 22 seconds creates an optimal surface by rounding edges without significantly altering average roughness (Sa) or peak-to-valley roughness (Sz). This balance between maintaining micro-compartments and softening peak structures could enhance osseointegration, as suggested by the increased core void volume (Vvc) and core height (Sk). These morphological changes facilitate better mechanical interlocking and biological integration of implants. The physicochemical surface characterization of the soft-edge microrough titanium, revealed significant findings. The SEM images showed that the machined titanium surfaces exhibited no discernible texture apart from the scratches from milling. In contrast, AFM profiling indicated that the peaks, which were sharp on the acid-etched surface, were effectively rounded after flame-heating, reducing the peak slopes, and increasing the inter-peak space. This was consistent with the reduced Sdq observed on the flame-heated surfaces. The XPS chemical analysis revealed that flame-heating reduced the percentage of surface oxygen and increased the surface carbon compared to the original acid-etched microrough surface. Wettability assessment indicated that both the knife-edge and soft-edge microrough surfaces

exhibited hydrophobic properties, with contact angles greater than 90°, whereas the machine-smooth surface was less hydrophobic with a contact angle greater than 60°.

The cytomorphometry analysis revealed that the area, perimeter, and Feret diameter of osteoblasts, which were notably reduced on the knife-edge microrough surfaces compared to the machine-smooth surfaces, were consistently restored on the soft-edge microrough surfaces. These improvements in cell morphology on the soft-edge surface suggest a more favorable environment for cell spreading and growth, which is crucial for successful osseointegration. These findings align with previous studies that emphasize the importance of surface topography in promoting cell adhesion and spreading. Boyan et al. (2002) demonstrated that osteoblast-mediated mineral deposition is highly dependent on surface microtopography, reinforcing our observations that improved cell morphology supports better osseointegration. Furthermore, the number of cells propagated until the subsequent culture day 4 was significantly higher on the soft-edge microrough surface compared to the knife-edge microrough surface, although still lower than on the machine-smooth surface. Microscopic images depicted extensive cell colonization and cluster formation on the soft edge microrough surface, indicating better cell proliferation. This observation is consistent with studies by Ogawa et al. (2003), which demonstrated that acid-etching enhances bone response. Our findings support that flame-heating can further optimize these roughness parameters to improve bone healing outcomes. The BrdU incorporation assay on day 4 confirmed that the cell proliferation rate on the soft-edge microrough surface increased compared to the knife-edge microrough surface, reaching a level equivalent to that on the machined surface. This is significant as it suggests that the soft-edge microrough surface can support cell proliferation to a similar extent as the smoother machined surface, while still maintaining the beneficial micro-compartmental

features. This supports previous study by Zhao et al. (2005) who showed that high surface energy and specific microstructures enhance cell response, which likely contributes to the improved proliferation rates observed on our flame-heated surfaces. Within 24 hours of seeding, the number of osteoblasts attached to the titanium surface was significantly lower on the original acid-etched microrough surface with knife-edges compared to the machine-smooth surface. However, this diminished cell attachment was significantly reversed on the soft edge microrough surface, as confirmed by fluorescent microscopic images. This suggests that the sharp peaks on the knife-edge surface may hinder cell attachment, while the rounded peaks on the soft-edge surface provide a more favorable environment for initial cell attachment. These findings align with the work of Zhao et al. (2005), who showed that high surface energy enhances cell response to titanium substrate microstructure, likely contributing to the improved attachment observed on our flame-heated surfaces.

Flow cytometric analysis of cell cycles on day 2 further supported these findings. The machine-smooth surface, associated with the most robust cell proliferation, exhibited the lowest percentage of cells in the G1 phase, while the knife-edge microrough surface, linked to the most suppressed cell proliferation, showed the highest percentage. The G1 phase percentage on the soft-edge microrough surface fell between these two extremes. The decrease in the percentage of cells in the S and G2 phases on the knife-edge microrough surface compared to the machine-smooth surfaces was mitigated on the soft-edge microrough surface. Consequently, osteoblasts on the soft-edge microrough surface displayed higher G2/G1 and S/G1 ratios than those on the knife-edge microrough surface, indicating a more favorable cell proliferation environment.

The analysis of osteoblast differentiation showed that total ALP activity was highest on the soft-edge microrough surface and lowest on the knife-edge microrough surface. When standardized by the number of cells, ALP activity and mineralized matrix formation were highest on the soft-edge microrough surface and lowest on the machine-smooth surface. The expression levels of osteoblastic differentiation marker genes were consistently higher on the microrough surfaces than on the machine-smooth surface, with no significant difference between the knife-edge and soft-edge microrough surfaces. These results indicate that osteoblast differentiation was not compromised and was even enhanced on the soft edge microrough surface compared to the knife-edge microrough surface, aligning with findings by Boyan et al. (2002).

In vivo osseointegration results showed that the biomechanical push-in test generated typical load-strain curves for both knife-edge and soft-edge microrough implants. Since Ogawa et al. (2000) demonstrated that push-in test values for machine smooth surfaces of implants were less than those for knife-edge surfaces, we built our research in accordance with these findings[54]. We found that the soft edge micro-rough surfaces exhibited significantly greater push-in test values than those with knife-edge surfaces throughout the experimental period. This finding emphasizes the influence of surface topography on osseointegration and the biomechanical stability of implants. The yield strength of osseointegration around soft edge microrough implants was approximately double that around knife-edge microrough implants. Additionally, the elastic modulus was 1.6 times higher for implants with soft-edge microrough surfaces, and the resiliency and energy of osseointegration were more than twice as high for the soft-edge microrough surfaces compared to the knife-edge microrough surfaces. SEM images of implants after the push-in test revealed extensive bone coverage around the soft-edge microrough surfaces, whereas only a limited area of

the knife-edge microrough surfaces exhibited remaining bone. This indicates that the surface retained a layer of mineralized tissue even after the rupture of osseointegration, suggesting cohesive fracture. These findings align with the work of De Maeztu et al. (2008), who showed that surface modifications can significantly enhance osseointegration.

Chapter 6 Conclusion

In conclusion, we were successful in optimizing surface morphology of titanium implants by utilizing the method of flame heating. This novel micro rough titanium surface significantly promoted osteoblast attachment and proliferation without compromising the differentiation and spreading of osteoblasts. The overall strength of osseointegration was optimum when the acid-etched Ti surface was fame heated for 22 secs. These modifications are likely to facilitate better mechanical interlocking and biological integration of implants. Our study provides a foundation for further research into the biological and mechanical benefits of this technique, potentially leading to improved clinical outcomes in dental and orthopedic implantology.

Bibliography:

[1] M. Weinlaender, E.B. Kenney, V. Lekovic, J. Beumer, 3rd, P.K. Moy, S. Lewis, Histomorphometry of bone apposition around three types of endosseous dental implants, Int J Oral Maxillofac Implants 7(4) (1992) 491-6.

[2] L. Chambrone, M.V. Rincon-Castro, A.E. Poveda-Marin, M.P. Diazgranados-Lozano, C.E. Fajardo-Escolar, M.C. Bocanegra-Puerta, L.F. Palma, Histological healing outcomes at the bone-titanium interface of loaded and unloaded dental implants placed in humans: A systematic review of controlled clinical trials, Int J Oral Implantol (Berl) 13(4) (2020) 321-342.

[3] T. Berglundh, I. Abrahamsson, J.P. Albouy, J. Lindhe, Bone healing at implants with a fluoride-modified surface: an experimental study in dogs, Clin Oral Implants Res 18(2) (2007) 147-52.

[4] T. Ogawa, I. Nishimura, Different bone integration profiles of turned and acid-etched implants associated with modulated expression of extracellular matrix genes, Int J Oral Maxillofac Implants 18(2) (2003) 200-10.

[5] M.A. De Maeztu, I. Braceras, J.I. Alava, C. Gay-Escoda, Improvement of osseointegration of titanium dental implant surfaces modified with CO ions: a comparative histomorphometric study in beagle dogs, Int J Oral Maxillofac Surg 37(5) (2008) 441-7.

[6] M. Bachle, R.J. Kohal, A systematic review of the influence of different titanium surfaces on proliferation, differentiation and protein synthesis of osteoblast-like MG63 cells, Clin Oral Implants Res 15(6) (2004) 683-92.

[7] G. Zhao, Z. Schwartz, M. Wieland, F. Rupp, J. Geis-Gerstorfer, D.L. Cochran, B.D. Boyan, High surface energy enhances cell response to titanium substrate microstructure, J Biomed Mater Res A 74(1) (2005) 49-58.

[8] B.D. Boyan, L.F. Bonewald, E.P. Paschalis, C.H. Lohmann, J. Rosser, D.L. Cochran, D.D. Dean, Z. Schwartz, A.L. Boskey, Osteoblast-mediated mineral deposition in culture is dependent on surface microtopography, Calcif Tissue Int 71(6) (2002) 519-29.

[9] K. Takeuchi, L. Saruwatari, H.K. Nakamura, J.M. Yang, T. Ogawa, Enhanced intrinsic biomechanical properties of osteoblastic mineralized tissue on roughened titanium surface, J Biomed Mater Res A 72A(3) (2005) 296-305.

[10] T. Ogawa, C. Sukotjo, I. Nishimura, Modulated bone matrix-related gene expression is associated with differences in interfacial strength of different implant surface roughness, J Prosthodont 11(4) (2002) 241-7.

[11] H. Aita, N. Hori, M. Takeuchi, T. Suzuki, M. Yamada, M. Anpo, T. Ogawa, The effect of ultraviolet functionalization of titanium on integration with bone, Biomaterials 30(6) (2009) 1015-25.

[12] H. Kitajima, K. Komatsu, T. Matsuura, R. Ozawa, J. Saruta, S.R. Taleghani, J. Cheng, T. Ogawa, Impact of nano-scale trabecula size on osteoblastic behavior and function in a meso-nano hybrid rough biomimetic zirconia model, J Prosthodont Res 67(2) (2023) 288-299.

[13] N.M. Rezaei, M. Hasegawa, M. Ishijima, K. Nakhaei, T. Okubo, T. Taniyama, A. Ghassemi, T. Tahsili, W. Park, M. Hirota, T. Ogawa, Biological and osseointegration capabilities of hierarchically (meso-/micro-/nano-scale) roughened zirconia, Int J Nanomedicine 13 (2018) 3381-3395.

[14] J. Saruta, R. Ozawa, T. Okubo, S.R. Taleghani, M. Ishijima, H. Kitajima, M. Hirota, T. Ogawa, Biomimetic Zirconia with Cactus-Inspired Meso-Scale Spikes and Nano-Trabeculae for Enhanced Bone Integration, Int J Mol Sci 22(15) (2021).

[15] N. Tsukimura, N. Kojima, K. Kubo, W. Att, K. Takeuchi, Y. Kameyama, H. Maeda, T. Ogawa, The effect of superficial chemistry of titanium on osteoblastic function, J Biomed Mater Res A 84(1) (2008) 108-16.

[16] T. Ueno, T. Ikeda, N. Tsukimura, M. Ishijima, H. Minamikawa, Y. Sugita, M. Yamada, N. Wakabayashi, T. Ogawa, Novel antioxidant capability of titanium induced by UV light treatment, Biomaterials 108 (2016) 177-86.

[17] F. Iwasa, N. Tsukimura, Y. Sugita, R.K. Kanuru, K. Kubo, H. Hasnain, W. Att, T. Ogawa, TiO2 micro-nano-hybrid surface to alleviate biological aging of UV-photofunctionalized titanium, Int J Nanomedicine 6 (2011) 1327-41.

[18] M. Yamada, T. Miyauchi, A. Yamamoto, F. Iwasa, M. Takeuchi, M. Anpo, K. Sakurai, K. Baba, T. Ogawa, Enhancement of adhesion strength and cellular stiffness of osteoblasts on mirror-polished titanium surface by UV-photofunctionalization, Acta Biomater 6(12) (2010) 4578-88.

[19] T. Ueno, M. Yamada, Y. Igarashi, T. Ogawa, N-acetyl cysteine protects osteoblastic function from oxidative stress, J Biomed Mater Res A 99(4) (2011) 523-31.

[20] T. Ueno, M. Yamada, T. Suzuki, H. Minamikawa, N. Sato, N. Hori, K. Takeuchi, M. Hattori, T. Ogawa, Enhancement of bone-titanium integration profile with UV-photofunctionalized titanium in a gap healing model, Biomaterials 31(7) (2010) 1546-57.

[21] F. Iwasa, N. Tsukimura, Y. Sugita, R.K. Kanuru, K. Kubo, H. Hasnain, W. Att, T. Ogawa, TiO2 micro-nano-hybrid surface to alleviate biological aging of UV-photofunctionalized titanium, International journal of nanomedicine 6 (2011) 1327-41.

[22] K. Hamajima, R. Ozawa, J. Saruta, M. Saita, H. Kitajima, S.R. Taleghani, D. Usami, D. Goharian, M. Uno, K. Miyazawa, S. Goto, K. Tsukinoki, T. Ogawa, The Effect of TBB, as an Initiator, on the Biological Compatibility of PMMA/MMA Bone Cement, Int J Mol Sci 21(11) (2020).

[23] K. Komatsu, T. Matsuura, T. Suzumura, T. Ogawa, Genome-wide transcriptional responses of osteoblasts to different titanium surface topographies, Mater Today Bio 23 (2023) 100852.

[24] T. Taniyama, J. Saruta, N. Mohammadzadeh Rezaei, K. Nakhaei, A. Ghassemi, M. Hirota, T. Okubo, T. Ikeda, Y. Sugita, M. Hasegawa, T. Ogawa, UV-Photofunctionalization of Titanium Promotes Mechanical Anchorage in A Rat Osteoporosis Model, Int J Mol Sci 21(4) (2020).

[25] T. Matsuura, K. Komatsu, D. Chao, Y.C. Lin, N. Oberoi, K. McCulloch, J. Cheng, D. Orellana, T. Ogawa, Cell Type-Specific Effects of Implant Provisional Restoration Materials on the Growth and Function of Human Fibroblasts and Osteoblasts, Biomimetics (Basel) 7(4) (2022).

[26] W. Att, N. Hori, F. Iwasa, M. Yamada, T. Ueno, T. Ogawa, The effect of UV-photofunctionalization on the time-related bioactivity of titanium and chromium-cobalt alloys, Biomaterials 30(26) (2009) 4268-76.

[27] J. Saruta, R. Ozawa, K. Hamajima, M. Saita, N. Sato, M. Ishijima, H. Kitajima, T. Ogawa, Prolonged Post-Polymerization Biocompatibility of Polymethylmethacrylate-Tri-n-Butylborane (PMMA-TBB) Bone Cement, Materials (Basel) 14(5) (2021).

[28] M. Ishijima, M. Hirota, W. Park, M.J. Honda, N. Tsukimura, K. Isokawa, T. Ishigami, T. Ogawa, Osteogenic cell sheets reinforced with photofunctionalized micro-thin titanium, J Biomater Appl 29(10) (2015) 1372-84.

[29] Y. Sugita, K. Ishizaki, F. Iwasa, T. Ueno, H. Minamikawa, M. Yamada, T. Suzuki, T. Ogawa, Effects of pico-to-nanometer-thin TiO2 coating on the biological properties of microroughened titanium, Biomaterials 32(33) (2011) 8374-84.

[30] M. Hasegawa, J. Saruta, M. Hirota, T. Taniyama, Y. Sugita, K. Kubo, M. Ishijima, T. Ikeda, H. Maeda, T. Ogawa, A Newly Created Meso-, Micro-, and Nano-Scale Rough Titanium Surface Promotes Bone-Implant Integration, Int J Mol Sci 21(3) (2020).

[31] K. Nakhaei, M. Ishijima, T. Ikeda, A. Ghassemi, J. Saruta, T. Ogawa, Ultraviolet Light Treatment of Titanium Enhances Attachment, Adhesion, and Retention of Human Oral Epithelial Cells via Decarbonization, Materials (Basel) 14(1) (2020).

[32] J. Saruta, N. Sato, M. Ishijima, T. Okubo, M. Hirota, T. Ogawa, Disproportionate Effect of Sub-Micron Topography on Osteoconductive Capability of Titanium, Int J Mol Sci 20(16) (2019).

[33] N. Kojima, S. Ozawa, Y. Miyata, H. Hasegawa, Y. Tanaka, T. Ogawa, High-throughput gene expression analysis in bone healing around titanium implants by DNA microarray, Clin Oral Implants Res 19(2) (2008) 173-81.

[34] N. Tsukimura, T. Ueno, F. Iwasa, H. Minamikawa, Y. Sugita, K. Ishizaki, T. Ikeda, K. Nakagawa, M. Yamada, T. Ogawa, Bone integration capability of alkali- and heat-treated nanobimorphic Ti-15Mo-5Zr-3Al, Acta biomaterialia 7(12) (2011) 4267-77.

[35] W. Att, N. Tsukimura, T. Suzuki, T. Ogawa, Effect of supramicron roughness characteristics produced by 1- and 2-step acid etching on the osseointegration capability of titanium, Int J Oral Maxillofac Implants 22(5) (2007) 719-28.

[36] T. Ogawa, S. Ozawa, J.H. Shih, K.H. Ryu, C. Sukotjo, J.M. Yang, I. Nishimura, Biomechanical evaluation of osseous implants having different surface topographies in rats, J Dent Res 79(11) (2000) 1857-63.

[37] S. Ozawa, T. Ogawa, K. Iida, C. Sukotjo, H. Hasegawa, R.D. Nishimura, I. Nishimura, Ovariectomy hinders the early stage of bone-implant integration: histomorphometric, biomechanical, and molecular analyses, Bone 30(1) (2002) 137-43.

[38] N. Tsukimura, M. Yamada, F. Iwasa, H. Minamikawa, W. Att, T. Ueno, L. Saruwatari, H. Aita, W.A. Chiou, T. Ogawa, Synergistic effects of UV photofunctionalization and micro-nano hybrid topography on the biological properties of titanium, Biomaterials 32(19) (2011) 4358-4368.

[39] Y. Sugita, T. Okubo, M. Saita, M. Ishijima, Y. Torii, M. Tanaka, C. Iwasaki, T. Sekiya, M. Tabuchi, N. Mohammadzadeh Rezaei, T. Taniyama, N. Sato, J. Saruta, M. Hasegawa, M. Hirota, W. Park, M.C. Lee, H. Maeda, T. Ogawa, Novel Osteogenic Behaviors around Hydrophilic and Radical-Free 4-META/MMA-TBB: Implications of an Osseointegrating Bone Cement, Int J Mol Sci 21(7) (2020).

[40] T. Ueno, N. Tsukimura, M. Yamada, T. Ogawa, Enhanced bone-integration capability of alkali- and heat-treated nanopolymorphic titanium in micro-to-nanoscale hierarchy, Biomaterials 32(30) (2011) 7297-308.

[41] T. Ueno, M. Yamada, N. Hori, T. Suzuki, T. Ogawa, Effect of ultraviolet photoactivation of titanium on osseointegration in a rat model, Int J Oral Maxillofac Implants 25(2) (2010) 287-94.

[42] I. Nishimura, Y. Huang, F. Butz, T. Ogawa, A. Lin, C.J. Wang, Discrete deposition of hydroxyapatite nanoparticles on a titanium implant with predisposing substrate microtopography accelerated osseointegration, Nanotechnology 18(24) (2007).

[43] Rupp, F., Gittens, R. A., Scheideler, L., Marmur, A., Boyan, B. D., Schwartz, Z., & Geis-Gerstorfer, J. (2014).
Surface characteristics of dental implants: A review. Dental Materials, 30(3), 288-306.

[44] Buser, D., Schenk, R. K., Steinemann, S., Fiorellini, J. P., Fox, C. H., & Stich, H. (1991).
Influence of surface characteristics on bone integration of titanium implants: A histomorphometric study in miniature pigs. Journal of Biomedical Materials Research, 25(7), 889-902.

[45] Cochran, D. L., Schenk, R. K., Lussi, A., Higginbottom, F. L., & Buser, D. (1998).

[46] Bone response to unloaded and loaded titanium implants with a sandblasted and acid-etched surface: A histometric study in the canine mandible. Journal of Biomedical Materials Research, 40(1), 1-11.

[47] Le Guéhennec, L., Soueidan, A., Layrolle, P., & Amouriq, Y. (2007).
Surface treatments of titanium dental implants for rapid osseointegration. Dental Materials, 23(7), 844-854.

[48] Albrektsson, T., & Wennerberg, A. (2004). Oral implant surfaces: Part 1—Review focusing on topographic and chemical properties of different surfaces and in vivo responses to them. The International Journal of Prosthodontics, 17(5), 536-543.

[49] Wennerberg, A., & Albrektsson, T. (2000). Suggested guidelines for the topographic evaluation of implant surfaces. The International Journal of Oral & Maxillofacial Implants, 15(3), 331-344.

[50] Long-term evaluation of non-submerged ITI implants. Part 1: 8-year life table analysis of a prospective multi-center study with 2359 implants. Clinical Oral Implants Research, 8(3), 161-172.

[51] Jemat, A., Ghazali, M. J., Razali, M., & Otsuka, Y. (2015).
Surface modifications and their effects on titanium dental implants. BioMed Research International, 2015, Article ID 791725.

[52] Variola, F., Brunski, J. B., Orsini, G., de Oliveira Fernandes, G. V., Nanci, A. (2011). Nanoscale surface modifications of medically relevant metals: State-of-the art and perspectives. Nanoscale, 3(2), 335-353.

[53] Gittens, R. A., Olivares-Navarrete, R., Schwartz, Z., & Boyan, B. D. (2014). Implant osseointegration and the role of microroughness and nanostructures: Lessons for spine implants. Acta Biomaterialia, 10(8), 3363-3371.

[54] Ogawa T, Ozawa S, Shih J-H, et al. Biomechanical Evaluation of Osseous Implants Having Different Surface Topographies in Rats. Journal of Dental Research. 2000;79(11):1857-1863.